2016

Characterisation of water sprays using high-speed videography

Alan Green
University of Wollongong, alang@uow.edu.au

Paul Cooper
University of Wollongong, pcooper@uow.edu.au

Trent D. Penman
Western Sydney University, tpenman@uow.edu.au

Ross A. Bradstock
University of Wollongong, rossb@uow.edu.au

Characterisation of water sprays using high-speed videography

Abstract

This paper reports on the characterisation of water sprays for the purpose of modelling the effectiveness of such sprays in mitigating the impacts of wildfires on residential buildings. Four types of water spray nozzles were experimentally tested and analysed using a single high-speed camera and image analysis software. The sprays were generated by a misting nozzle, a hollow-cone nozzle, a rotating 'butterfly' sprinkler and a deflector plate sprinkler. Back-illumination was used to produce silhouette images of droplets within each spray. The point spread function half-width of each droplet image was determined, to give an indication of the distance of the droplet from the focal plane. In this way a control volume was defined for the measurements without introducing a bias towards larger or smaller droplets. The high-speed videos were analysed using a custom-built script in the software Matlab. Overlapping droplet images were identified through the high spatial rate of change of grey-level gradient around their perimeters. These images were separated, reconstructed and corrected for any resulting change in local contrast. The size of each droplet was measured and the velocities of individual droplets were determined by tracking the droplets between video frames. Results are presented on the spatial distribution of droplet sizes and velocities within each spray in terms of probability density functions. Commentary is also provided on how this data will be used in future computational fluid dynamics analyses of sprays implemented on the exterior of residential buildings and the effects of wind thereon.

Characterisation of Water Sprays using High-Speed Videography

A. Green[1], P. Cooper[1], T. Penman[2] and R. Bradstock[3]

[1]Sustainable Buildings Research Centre, University of Wollongong, Wollongong, New South Wales 2522, Australia

[2] Ecosystem and Forest Sciences, University of Melbourne, Melbourne, Victoria 3010, Australia

[3]Centre for Environmental Risk Management of Bushfires, University of Wollongong, Wollongong, New South Wales 2522, Australia

Abstract

This paper reports on the characterisation of water sprays for the purpose of modelling the effectiveness of such sprays in mitigating the impacts of wildfires on residential buildings. Four types of water spray nozzles were experimentally tested and analysed using a single high-speed camera and image analysis software. The sprays were generated by a misting nozzle, a hollow-cone nozzle, a rotating 'butterfly' sprinkler and a deflector plate sprinkler. Back-illumination was used to produce silhouette images of droplets within each spray. The point spread function half-width of each droplet image was determined, to give an indication of the distance of the droplet from the focal plane. In this way a control volume was defined for the measurements without introducing a bias towards larger or smaller droplets. The high-speed videos were analysed using a custom-built script in the software Matlab. Overlapping droplet images were identified through the high spatial rate of change of grey-level gradient around their perimeters. These images were separated, reconstructed and corrected for any resulting change in local contrast. The size of each droplet was measured and the velocities of individual droplets were determined by tracking the droplets between video frames. Results are presented on the spatial distribution of droplet sizes and velocities within each spray in terms of probability density functions. Commentary is also provided on how this data will be used in future computational fluid dynamics analyses of sprays implemented on the exterior of residential buildings and the effects of wind thereon.

Introduction

The characterisation of liquid sprays is an area of keen interest for researchers in a variety of fields, ranging from rocket design to ink-jet printer development. For many practical applications, the complex mechanisms by which a spray is formed from a bulk fluid is of less interest than the eventual characteristics of the spray after formation. Spray characterisation often aims to develop a representation of the droplet diameters and velocities some distance beyond the primary breakup region. The level of detail that these representations include depends on the application. Some simple purposes require only a mean droplet diameter (often the volume-weighted mean diameter, d_{43}, or Sauter mean diameter, d_{32}), while more detailed work such as computational fluid dynamics (CFD) simulations can benefit from having information on the spatial and temporal distributions of droplet diameters and velocities within a spray.

Common techniques for the experimental measurement of these distributions include laser diffraction, laser Doppler anemometry, phase Doppler interferometry and a range of image-based methods, e.g. laser-induced fluorescence particle sizing, particle image velocimetry (PIV) and particle tracking velocimetry (PTV). Advantages of the image-based techniques include their ability to

measure a large region of a given spray and that they produce images which give qualitative insights into the spray behaviour, in addition to quantitative measurements. They can also typically measure non-spherical droplets much more accurately [8], which makes them more suitable for the measurement of sprays with large droplets.

A disadvantage of image-based techniques is the inherent difficulty in the determination of droplet locations in a third dimension, normal to the image plane. To overcome this challenge, the spray can be observed from more than one angle using multiple cameras, the spray can be illuminated with a thin, lateral sheet of light [12], or criteria can be applied during image post-processing to eliminate droplets which were outside of a known depth of field (DOF) [1-3,6,9,10]. One such DOF criterion has been developed and applied to fuel sprays by Blaisot et al. [1,2,6,10]. It sets a maximum value for the point-spread function (PSF) half-width—a measure of the 'blurriness' of an image—with which droplet images are included in the measurement. The main advantage of this approach is that it does not introduce a bias towards larger or smaller droplets.

In this study, sprays were characterised using an image-based method which incorporates the maximum PSF half-width DOF criterion. The sprays are typical of those used to protect residential buildings from wildfires (a.k.a. bushfires or forest fires); spray systems used for this purpose generally incorporate residential irrigation sprinklers of various designs [7,11]. The sprays studied here represent a number of these different sprinkler designs and, as a result, exhibit a range of droplet sizes, velocities and spray patterns, including periodic behaviour. The focus here is to outline the combinations of new and established methods which were found to be useful in the characterisation of these sprays.

Method

Four sprays were selected for analysis, which were produced by a Tecpro KHW-1390 180° flat-fan misting nozzle, a ½" Champion S9F hollow-cone nozzle, a Holman ½" 'butterfly' sprinkler and a Lechler 525.049 deflector-plate spray head. These sprays are hereafter referred to as sprays M, HC, B and DP, respectively. Some details of the sprays and their measurement are presented in table 1. The nozzles were new at the time of measurement.

Video Acquisition

Each of the sprays was operated individually within a 3m × 1.8m × 2.4m (high) enclosure. The enclosure was used to contain water from the sprays, recirculate it to the supply pump and to exclude light other than that which was introduced as back-lighting. A pressure regulator was installed 2m upstream of the spray nozzles. The water pressure directly downstream of the regulator was monitored and maintained within ±5% of the values reported in

table 1 while the sprays were videoed. The pressure drop between the pressure sensor and the nozzle being measured is estimated to have contributed an additional error of less than 3%.

		M	HC	B	DP
Spray Details	Pressure (kPa)	400	345	200	245
	Flow rate (L/min)	4.1	12.5	33.9	41.8
	d_{43} (μm)	335	630	715	595
Camera & Optics	Working distance (mm)	122	122	247	247
	Scale (px/mm)	50.53	50.53	22.42	22.42
	Field of view (mm) (width; height)	13.9; 13.9	25.3; 15.8	57.1; 35.7	57.1; 35.7
	Frame rate (frames/s)	11,104	6,273	6,273	6,273
	Exposure length (μs)	4	7	7	5
Measurements	Number of measurement regions	160	23	24	22
	Number of droplets sampled ($\times 10^3$)	222	103	651	200
	Portion of droplets inside DOF (%)	76.7	46.0	16.5	21.6

Table 1. Details of the sprays generated by the misting nozzle (M), hollow-cone nozzle (HC), butterfly sprinkler (B) and deflector-plate nozzle (DP).

Back-illumination was provided to the sprays by four 185W LED lights. A constant voltage was supplied to the lights to avoid flicker in the high-speed footage. The lights were positioned outside the test enclosure and shone through a diffuser in one of the enclosure walls. The sprays were videoed through a window on the opposite wall of the enclosure, so as to produce silhouette images of droplets within the sprays. A single Vision Research Phantom v611 high-speed camera with colour sensor was used, fitted with a Tamron 90mm f/2.8 macro lens.

The sprays were each measured at a working distance of either 122mm or 247mm, depending on the sizes of droplets which needed to be resolved and the amount of visual interference caused by water impinging on the window through which the camera viewed the sprays. Videos were recorded for a number of regions within each spray, beyond the primary breakup region. The measurement regions were typically overlapping and coplanar, so as to measure the spray throughout a plane. Sprays HC and DP were assumed to be axisymmetric and so only one plane was measured within these sprays. The rotating deflector on the butterfly sprinkler gave spray B an unsteady, swirling character, which was also assumed to be axisymmetric when time-averaged, so it too was only measured through one plane. Spray M was clearly not axisymmetric but was assumed to be symmetric about a central plane. Videos were recorded through a number of planes on one side of the plane of symmetry, resulting in a substantially higher number of measurement locations.

Model Calibration and Verification

Videos were also recorded at both working distances of individual droplets of five known diameters and a series of eight opaque discs etched on a glass slide, with the droplets and slide positioned at a range of known distances in front of and behind the focal plane. The images were used to assess the applicability of the theoretical models for diameter correction and PSF half-width calculation which are presented in [6] and [1], respectively. The images were also used to determine the relationship between PSF half-width and out-of-focus distance.

Image Analysis

Images of the sprays were analysed using a custom-built script for Matlab software (version R2016a). Individual video frames were analysed and the droplets which were identified and measured within them were tracked between frames in an automated process. The method adopted for the analysis of each frame was modelled closely on that of Blaisot et al. [1,2,6,10], with adjustments to suit the large, often non-spherical droplets in the present sprays.

The frame being analysed was first normalised following the procedure reported in [6] and converted to grey-scale. Droplet images were located within each frame using a grey-level intensity threshold of 0.3, and by convoluting the image with three inverted 'Mexican hat' (i.e. Laplacian of Gaussian) wavelet functions. The union of regions identified by these methods gave a collection of regions (or 'blobs') which correlated with regions within the frame that were dark or had a high concavity in the grey-level intensity profile. Any of these blobs which touched the border of the frame or were comprised of less than 3 pixels were disregarded, to avoid any incomplete droplet images or noise from being included in the measurement.

Each of the droplet images which correlated to the remaining blobs was then analysed individually, as is shown in figure 1. A sub-pixel, bilinear interpolation was performed on a region encompassing the droplet image, improving the precision with which the droplet outline could be defined. A local contrast value was calculated for the droplet image by the method reported in [6] and the boundary of the droplet was defined as the contour of 0.5 relative level (i.e. the contour where the grey-level intensity was half-way between the minimum and background intensities of the image).
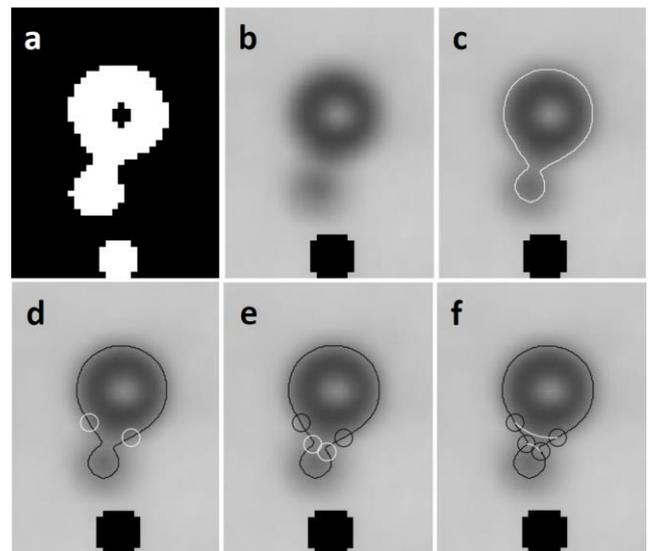

Figure 1. Images showing a number of the steps in the analysis of each 'blob' within a video frame: (a) the blob and surrounding region which was to be analysed; (b) the corresponding droplet image after sub-pixel interpolation and with surrounding blobs masked; (c) the droplet outline as determined from a local contrast value and relative level of 0.5; (d) points of high spatial rate of change of grey-level gradient on the droplet image outline, which were identified as break points between two overlapping droplet images; (e) secondary break points for the reconstruction of the droplet image which was in poorer focus; and (f) arcs drawn to reconstruct the two droplet outlines.

An analysis was then performed to determine whether the droplet image was likely to be comprised of overlapping images of more than one droplet. The grey-level gradient was measured at each pixel on the outline of the droplet image and a smoothing spline was fitted to this gradient data. Peaks in the absolute value of the derivative of this spline correlated to points at which the rate of change of grey-level gradient along the image outline was high. If these peaks were over a set value the corresponding point was considered a potential 'break point'. Droplet images with two or more potential break points were determined to be the overlapping images of two or more droplets and were treated as a number of separate droplets in further analysis. The break points generated by this method were found to lie closer to the droplet image which

was in sharper focus (see, e.g., image d in figure 1). Secondary break points were defined a distance of $0.67s_{PSF}$ along the outline of the droplet, from each original break point, towards the less focused of the two droplet images; here s_{PSF} is the PSF half-width of the droplet image which is in poorer focus. Each droplet outline was then reconstructed with an arc, the radius of which depended on the chord length and the perimeter of droplet outline between the break points.

The equivalent spherical diameter of the droplet was then estimated by dividing the region inside the droplet outline into a number of slices, assuming each slice to represent a disc and summing the volumes of these discs, as in [2]. The mean grey-level gradient at the outline of the droplet image was also measured. Empirical models, which were developed during the calibration procedure described above, were used to correct the measured diameter, calculate the droplet image PSF half-width from the measured gradient and estimate the distance of the droplet from the focal plane using this PSF half-width.

Droplet Tracking

Droplets were tracked between video frames using a procedure similar to that reported by Dalziel [5], and implemented for PTV in the 'Digiflow' software [4]. The pairing of droplets from one frame to those of a subsequent frame was formulated as a cost-minimisation problem. A 'cost' was calculated for the pairing of each droplet in one frame to those in the other. These costs were calculated as a function of the difference in size and out-of-focus distance between the two droplets, as well as the distance between the droplet in the second frame and the predicted location of the droplet from the first frame. A cost was also set for the pairing of any of the droplets with a hypothetical 'out-of-frame' droplet; this cost was included to allow droplets which were only present in one of the frames being considered to not interfere with the tracking of others. The final pairing of droplets minimised the sum total cost and was reached iteratively. The analysis of a sequence of frames ultimately determined a number of droplet 'tracks'. The mean diameter, out-of-focus distance, location and velocity of each track represented a single data entry for further analysis.

In order to resolve the temporal variations in spray B, sequences of images were analysed that were only five frames in length. These samples were taken at a frequency 12 times that of the dominant spray frequency, giving tracks that could be associated with various stages of the spray's development in time.

Spray Characterisation

In order to characterise each spray, data from all measurement locations was subjected to a five-step process: (1) spurious tracks were neglected (e.g. tracks spanning only two frames and those with a high coefficient of variation in the distances travelled between frames); (2) droplets that were suspected to have been re-entrained into the spray, rather than to have originated directly from the spray nozzle, were neglected (criteria included limits on the droplet direction of travel and a minimum speed threshold, which was a function of diameter and represented the speed with which a droplet of a given diameter would reach the measurement location if it had originated from the nozzle); (3) droplets outside of a set DOF were neglected (DOFs of 3mm and 6mm were set for measurements taken at working distances of 122mm and 247mm, respectively); (4) hypothetical initial velocities were calculated for each measured droplet, representing the velocities with which they would have left the nozzle if it were a point source of non-interacting droplets (i.e. if no breakup region existed); (5) multivariate probability density functions (PDFs) were fitted to the resulting data using a kernel density estimation method with Gaussian kernels. The PDFs for sprays HC and DP were defined in three dimensions: droplet diameter, speed and elevation angle. An additional dimension was included in the PDFs for spray M

(which was not assumed to be axisymmetric, so required a dimension representing the azimuthal angle) and spray B (which required phase angle to be included in order to resolve changes in the spray behaviour over time). Note that the phase angle included in PDFs for spray B could equally be considered as an azimuthal angle within a rotating coordinate system.

Results and Discussion

As was the case in previous studies [1,2,6], the theoretical model for diameter correction reported in [6] was found to perform poorly in practice. As in these other studies, an empirical alternative was developed for the specific optical arrangement being used. The measurement of the diameters of discs and droplets with this empirical model was found to be accurate within a limited DOF (see figure 2 and figure 3, respectively). Outside of this DOF the results became much less accurate; however this was not of great concern, since droplets outside a narrow DOF were to be neglected when analysing images of the sprays. Some parallax error was also observed. The use of a telecentric lens could have avoided this [6], however the macro lens used here introduced an error of less than 3.5%.
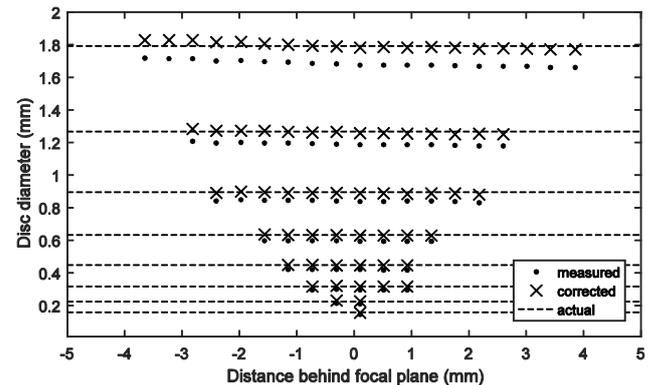

Figure 2. Raw and corrected measurements of the diameters of opaque discs at various distances in front of and behind the focal plane, at a working distance of 122mm.
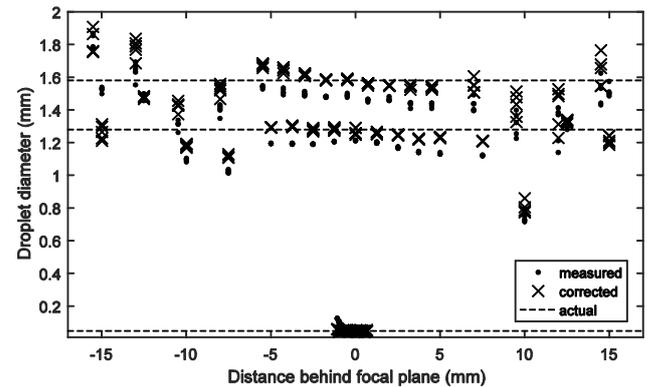

Figure 3. Raw and corrected measurements of the equivalent spherical diameter of droplets at various distances in front of and behind the focal plane, at a working distance of 122mm.

The theoretical model for the determination of a droplet image PSF half-width [1] was found to produce good results. PSF half-widths determined for images of droplets and discs of all sizes increased linearly with increasing distance from the focal plane. This data was used to define a relation between PSF half-width and out-of-focus distance for each working distance.

The technique for separation of overlapping droplet images reported here was found to be more effective than established methods based on watersheds and the curvature of the image outline [1-3,6,9] . This was especially true for the large, often non-spherical droplets found in sprays B and DP. However, careful

tuning of the script was required for each spray to minimise the number of droplet images that were split needlessly and those that should have been split but were overlooked.

The distribution of droplet diameters and speeds were compared from the PDFs for each spray (see figure 5 and figure 6, respectively). Spatial (and in the case of spray B, temporal) distributions of parameters could also be observed (e.g. see figure 7), as could correlations between parameters.
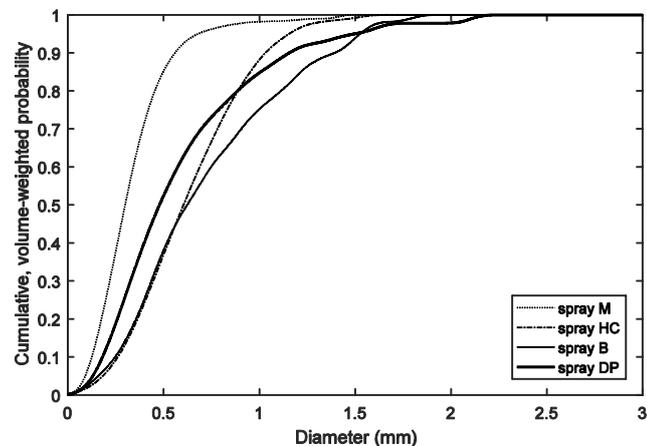

Figure 5. Cumulative, volume-weighted droplet diameter distributions for each of the sprays. Values within this plot indicate the portion of the spray flow which is contained in droplets with diameters less than a given value.
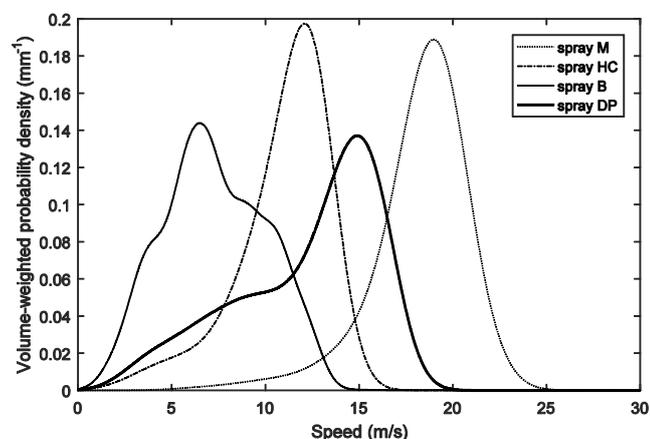

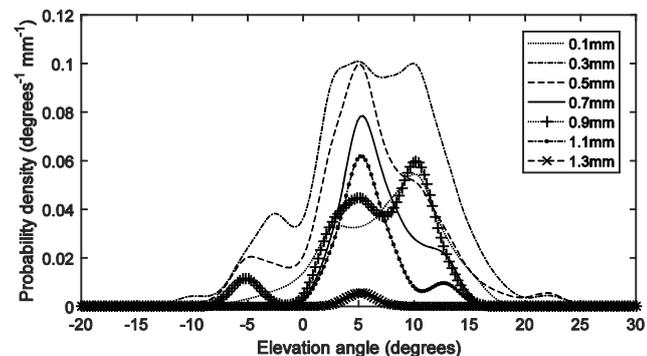Figure 6. Volume-weighted droplet speed distributions for droplets in each of the sprays.

Figure 7. An example of the multidimensional information contained in the spray PDFs: the volume-weighted PDF representing spray DP, integrated over all droplet speeds and shown for a number of droplet diameters.

PDFs produced in this study are to be used to produce boundary conditions for future CFD simulations. By discretising a PDF into the desired number of classes, point-sources of either Lagrangian parcels or Eulerian phases can be created to give an accurate representation of the spray.

Conclusions

Four water sprays were characterised using a back-lit, single-camera, high-speed videography technique, and the resulting sequences of images were analysed using a maximum PSF half-width DOF criterion and cost-function-based particle tracking algorithm. The separation of overlapping droplet images was achieved by a new method using the grey-level gradient at the perimeter of the droplet image. This method was found to be more effective than a number of previously established methods, especially for sprays containing large, non-spherical droplets. Overall, the combination of these methods proved to be a relatively simple and inexpensive way to gather detailed data on the sprays. Multivariate PDFs fitted to the data using a kernel density estimation method provided a comprehensive characterisation of each spray in terms of a point source of non-interacting droplets. Boundary conditions for future CFD simulation of such sprays can be readily obtained by discretising the PDFs into the desired number of particle or phase classes.

Acknowledgments

References

[1] Blaisot, J., Drop Size and Drop Size Distribution Measurements by Image Analysis, Heidelberg, Germany, 2012.

[2] Blaisot, J.B. & Yon, J., Droplet Size and Morphology Characterization for Dense Sprays by Image Processing: Application to the Diesel Spray, *Exp Fluids*, **39**(6), 2005, 977-994.

[3] Castanet, G. et al., High-Speed Shadow Imagery to Characterize the Size and Velocity of the Secondary Droplets Produced by Drop Impacts onto a Heated Surface, *Exp Fluids*, **54**(3), 2013, 1-17.

[4] Dalziel, S., Digiflow User Guide, Version 1.2, DL Research Partners, 2006.

[5] Dalziel, S.B., Decay of Rotating Turbulence: Some Particle Tracking Experiments, *Applied scientific research*, **49**(3), 1992, 217-244.

[6] Fdida, N. & Blaisot, J.B., Drop Size Distribution Measured by Imaging: Determination of the Measurement Volume by the Calibration of the Point Spread Function, *Measurement Science and Technology*, **21**(2), 2010, 025501.

[7] FPAA, External Water Spray Systems to Aid Building Protection from Wildfire, Fire Protection Association Australia, 2000.

[8] Frohn, A. & Roth, N., *Dynamics of Droplets*, Springer Science & Business Media, 2000.

[9] Kashdan, J.T., Shrimpton, J.S. & Whybrew, A., A Digital Image Analysis Technique for Quantitative Characterisation of High-Speed Sprays, *Optics and Lasers in Engineering*, **45**(1), 2007, 106-115.

[10] Malot, H. & Blaisot, J.-B., Droplet Size Distribution and Sphericity Measurements of Low-Density Sprays through Image Analysis, *Particle & Particle Systems Characterization*, **17**(4), 2000, 146-158.

[11] Potter, M. & Leonard, J., Spray System Design for Ember Attack, CSIRO - Sustainable Ecosystems, 2010.

[12] Putorti, A.D., Everest, D. & Atreya, A., Simultaneous Measurements of Drop Size and Velocity in Large-Scale Sprinkler Flows Using Particle Tracking and Laser-Induced Fluorescence, *Ann Arbor*, **1001**, 2004, 48109-2125.